Electronic mechanism of the surface enhanced Raman scattering

Hiromi Nakai and Hiroshi Nakatsuji[a)]
Department of Synthetic Chemistry and Biological Chemistry, Faculty of Engineering, Kyoto University, Sakyo-ku, Kyoto 606-01, Japan

(Received 23 December 1994; accepted 2 May 1995)

Electronic mechanism of the surface enhanced Raman scattering (SERS) is investigated by an *ab initio* molecular orbital theory. The time-dependent Hartree–Fock method is used to calculate the polarizability of the surface–molecule interacting system. For representing the surface effect, we use small solid clusters Ag_2, Ag_{10}, K_2, Pd_2, and MgO. The present method succeeds in describing the enhancement of the Raman intensity for the adsorbed CO molecule. The maximum intensity of the $Ag_{10}CO$ system is calculated to be seven orders of magnitude larger than that of the free CO molecule. Furthermore, the wavelength dependence of the Raman intensity calculated by the $Ag_{10}CO$ system agrees with the experimental spectrum. The electronic mechanism of the SERS is due to the resonance transitions, in which the surface polarization and the surface–molecule interaction are very important. This mechanism explains the orientation- and distance-dependencies in the surface–adsorbate interacting systems. © *1995 American Institute of Physics.*

I. INTRODUCTION

Since Fleischmann *et al.*[1] reported a Raman signal from pyridine adsorbed on a silver surface, where the intensity was enhanced by six orders of magnitude with respect to the free molecule, the surface enhanced Raman scattering (SERS) has been very widely used and aroused great interest in chemistry, physics, and material science. Some excellent review articles[2–6] have been published to discuss the various aspects of the SERS and to explain two separate mechanisms, namely, electromagnetic (EM) and charge-transfer (CT) mechanisms.

In the EM mechanism, the induced surface plasmon excitations, for which the surface roughness seems important, at or near the resonance give rise to an electric field enhancement. Since the typical EM models treat the adsorbed molecule as a simple dipole or ignore it completely in accounting for the response of the metal surface, they cannot distinguish the difference of the adsorbed molecule. Furthermore, the dipole approximation fails when the molecule has a short-range interaction with the surface. In fact, many theoretical studies show that the short-range chemical bond is essential for the chemisorption.[7]

On the other hand, the CT theory uses the specific ionized or affinity level of the free molecule. Namely, the basic idea is the resonance scattering caused by the CT transition between the surface and the admolecule, since for the free molecule no electronic transitions exist in the spectral region. However, this treatment cannot explain the differences due to the orientation of the adsorbed molecule and the distance from the surface, since the interaction between the surface and the molecule is not taken into account.

In the present study, we calculate the Raman intensities of the surface–molecule interacting systems by an *ab initio* molecular orbital (MO) theory. The polarizabilities of the gas-phase and the adsorbed CO molecules are calculated by the time-dependent Hartree–Fock (TDHF) method,[8–11] and the polarizability derivatives with respect to the C–O distance are calculated by the finite difference method. We will show that the enhancement of the Raman intensity of the adsorbed molecule is described by the present method. We analyze the electronic mechanism of the SERS due to the resonance transition, in which the surface polarization and the surface–molecule interaction are important. This mechanism explains the orientation- and distance-dependencies of the adsorbed molecule.

II. COMPUTATIONAL METHOD

The Raman scattering is a two-photon process, which is described by the second-order perturbation theory for the interacting Hamiltonian between electron and radiation field. The intensity is given by the so-called Kramers–Heisenberg–Dirac (KHD) dispersion equation,[12,13]

$$I_{mn}=\frac{128\pi^5}{9c^4} I_0(\nu_0+\nu_m-\nu_n)^4\sum_{\rho,\sigma}|a_{\rho\sigma}|^2, \tag{1}$$

where I_0 is the intensity of the incident light, ν_0 is its frequency, I_{mn} is the intensity of the scattered light with the transition from vibronic state $|m\rangle$ to $|n\rangle$, $(\nu_0+\nu_m-\nu_n)$ is its frequency, and c is the velocity of light. The sum goes over $\rho, \sigma=x, y, z$ independently. The $\rho\sigma$th matrix element of the polarizability tensor for the transition $|m\rangle\rightarrow|n\rangle$, $(a_{\rho\sigma})_{mn}$, is given by

$$a_{\rho\sigma}=\sum_{e\neq m,n}\left\{\frac{\langle m|D_\sigma|e\rangle\langle e|D_\rho|n\rangle}{h(\nu_e-\nu_m-\nu_0)-i\Gamma_e}+\frac{\langle m|D_\rho|e\rangle\langle e|D_\sigma|n\rangle}{h(\nu_e-\nu_n+\nu_0)-i\Gamma_e}\right\}, \tag{2}$$

where h is Planck's constant, D_ρ the ρth component of the electric moment operator, and Γ_e the damping constant, which is related to the life time τ_e of the intermediate state $|e\rangle$ by

[a)]Also at the Institute for Fundamental Chemistry, 34-4, Takano-Nishihirakicho, Sakyo-ku, Kyoto 606, Japan.

 0021-9606/95/103(6)/2286/9/$6.00 © 1995 American Institute of Physics

$$\tau_e \approx \frac{\hbar}{\Gamma_e}. \tag{3}$$

For the vibration Raman scattering, the polarizability tensor is related to the derivative of the molecular polarizability with respect to the normal coordinates x_j, which is called Placzek's polarizability approximation,[14]

$$a_{\rho\sigma} = \frac{1}{\sqrt{2}} \lambda_j \left(\frac{\partial \alpha_{\rho\sigma}}{\partial x_j} \right), \tag{4}$$

where $\alpha_{\rho\sigma}$ is the $\rho\sigma$ component of the polarizability tensor, which is calculated from the electronic wave function in the Born–Oppenheimer (BO) approximation, and λ_j corresponds to the amplitude of the normal mode x_j, which is the function of the mass and the frequency of the mode.

In the present study, the polarizability tensor of the surface–molecule interacting system is calculated by the *ab initio* molecular orbital (MO) method, and the polarizability derivative with respect to the vibrational coordinate is calculated using a finite difference approximation. The polarizability in Eq. (4) depends on the frequency of the incident light and on the damping constant. We use the time-dependent Hartree–Fock (TDHF) method,[8–11] especially the random-phase-approximation (RPA) formula developed by Pandey and Schatz,[11] to evaluate the frequency-dependent polarizabilities (FDPs).

In the TDHF theory, the first-order perturbed MOs $C^{(\pm)}$ are coupled with the unperturbed MOs $C^{(0)}$ as

$$\mathbf{C}^{(\pm)} = \frac{1}{2} \mathbf{C}^{(0)} \mathbf{A}^{(\pm)}, \tag{5}$$

where $A^{(\pm)}$ is a matrix of mixing coefficients and is determined by solving the following RPA-like equation,

$$\begin{bmatrix} \mathbf{M}^{11} & \mathbf{M}^{12} \\ \mathbf{M}^{21} & \mathbf{M}^{22} \end{bmatrix} \begin{bmatrix} \mathbf{A}^{(+)} \\ \mathbf{A}^{(-)} \end{bmatrix} = \begin{bmatrix} \mathbf{J}^{(+)} \\ \mathbf{J}^{(-)} \end{bmatrix}, \tag{6}$$

where

$$J_{ki}^{(\pm)} = -2H_{ki}^{(1)} / (\epsilon_k + i\Gamma_k - \epsilon_i \pm \hbar\omega), \tag{7}$$

$$M_{ki,k'i'}^{ab} = \delta_{ab}\delta_{kk'}\delta_{ii'} + [2/(\epsilon_k + i\Gamma_k - \epsilon_i \pm \hbar\omega)] R_{ki,k'i'}^{ab} \tag{8}$$

in which the indices i, k, etc. are the MO labels, $H^{(1)}$ the dipole matrix in the MO basis, ϵ the orbital energy obtained by the unperturbed HF calculation, Γ the damping constant, and ω the wave number of the electric field, which corresponds to that of the incident light in the Raman scattering. The superscripts a, b, run 1 and 2, which indicate the element of the matrix M. In Eq. (8), the + (plus) sign is for $a=1$ and − (minus) sign for $a=2$. R^{ab} is the difference between the two-electron integrals in the MO basis given by

$$R_{ki,k'i'}^{ab} = \begin{cases} (ki|i'k') - \frac{1}{2}(kk'|i'i) & (a=b), \\ (ki|k'i') - \frac{1}{2}(ki'|k'i) & (a \neq b). \end{cases} \tag{9}$$

By determining $A^{(\pm)}$ from Eq. (6), we get the FDP in the TDHF approximation as

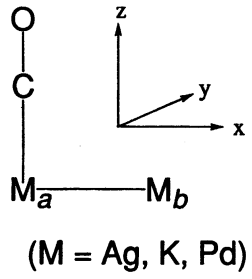

FIG. 1. Geometry of the M_2CO (M=Ag, K, Pd) systems.

$$\alpha(\omega) = -\sum_{i}^{\text{occ}} \sum_{k}^{\text{vac}} [A_{ki}^{(-)} + A_{ki}^{(+)}] H_{ki}^{(1)}. \tag{10}$$

We adopt an orbital selection scheme similar to the method of Pandey and Schatz; namely, we use only the unoccupied and occupied orbital pairs, k and i, which satisfy

$$\left| \frac{[H_{ki}^{(1)}]^2}{\epsilon_k - \epsilon_i \pm \hbar\omega} \right| \geq \eta \left| \frac{[H_{k'i'}^{(1)}]^2}{\epsilon_{k'} - \epsilon_{i'} \pm \hbar\omega} \right|_{\max}, \tag{11}$$

where the pair, k' and i', gives the maximum element of $|H_{ki}^2/(\epsilon_k - \epsilon_i \pm h\omega)|$ and η is a coefficient which depends on the desired accuracy. In this study, η is set to be 1.0×10^{-6}. Furthermore, the lowest two MOs corresponding to the $1s$ orbitals of O and C are frozen in the TDHF calculations.

We study CO molecule interacting with Ag_2, Ag_{10}, K_2, and Pd_2 as models of the adsorbed system. As illustrated in Fig. 1, CO is assumed to interact with M_2 in an end-on form. In Sec. III C, we use the Ag_{10} cluster as a more realistic model. The M–M bond lengths are fixed at the lattice constants of the crystals, namely, 2.8894, 4.6185, and 2.5711 Å for Ag–Ag, K–K, and Pd–Pd lengths, respectively.[15] The C–O bond lengths of 1.10 and 1.11 Å are used for calculating the polarizability derivative. We also calculated MgO(CO) and ArCO for investigating the effects of the metal oxide, MgO and the Ar matrix, respectively.

The zeroth-order MOs and the orbital energies are calculated with the use of the program HONDO7.[16] The Gaussian basis sets for the valence electrons of the Ag and Pd atoms are represented by the $[3s2p2d]$ sets and the Kr cores are replaced by the effective core potentials (ECPs).[17] We use the $[4s2p]$ sets and ECP for K.[18] All electron basis sets of Huzinaga[19] are used for Mg and Ar, two p functions (0.143, 0.045) are added to the former and two s and p functions (0.040 201, 0.017 125) and two d ones (0.950,0.263) are added to the latter. For the C and O atoms, we use $(9s5p)/[4s2p]$ set of Huzinaga–Dunning[20] augmented by the polarization d functions of $\alpha=1.154$ and 0.600, respectively.[19]

III. RESULTS AND DISCUSSIONS

A. Free CO and clusters

We first examine the polarizability of the free CO molecule and its derivative with respect to the C–O distance. Figure 2(a) shows the parallel and perpendicular components, $\alpha_\parallel$ and $\alpha_\perp$, of the CO polarizabilities as a function of the incident photon energy. As seen in Eqs. (1) and (2), the

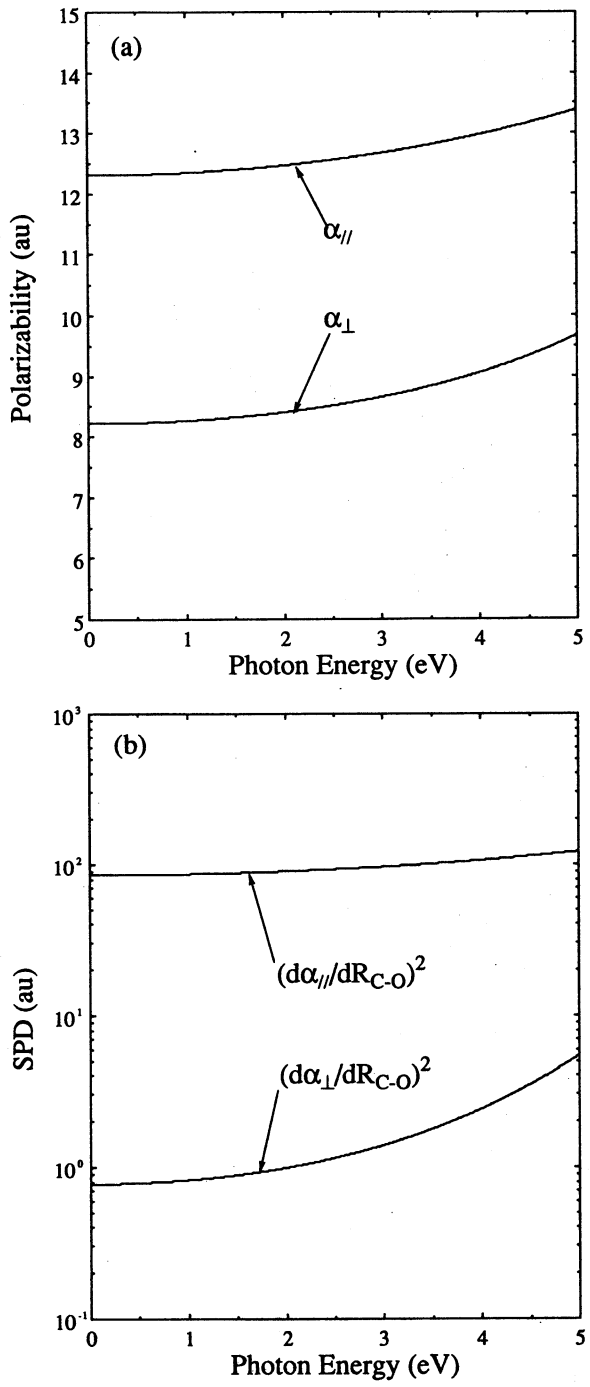

FIG. 2. (a) Frequency dependence of the polarizability and (b) the square of the polarizability derivative of the free CO molecule calculated by the TDHF method.

Raman intensity is proportional to the square of the polarizability derivative (SPD), of which the energy (or frequency) dependency is also shown in Fig. 2(b). In this energy region, both polarizability and SPD change only a little as shown in Fig. 2. Since the parallel SPD is by two orders of magnitude larger than the perpendicular one, the Raman intensity is mainly determined by the former.

Figure 3 shows the FDPs, $\alpha_{\parallel}$ and $\alpha_{\perp}$, of the free Ag_2, Pd_2, K_2, and MgO molecules, and the values of $\alpha_{\parallel}$ and $\alpha_{\perp}$ at $h\omega=1.0$ eV are shown in Table I. Generally speaking, the divergence of the FDP is due to the resonance with the excited state, and in the TDHF calculations the excitation energy is in the single-excitation configuration-interaction (SECI) approximation. The corresponding excited states and the SECI energies are shown in Table I. The $^1\Sigma$ and $^1\Pi$ states are related to the divergences of the parallel and perpendicular FDPs, respectively.

We perform an analysis of the FDP with Eq. (10). Table I shows the occupied and unoccupied orbital pair, $i\rightarrow k$, which mainly contributes to the FDP in Eq. (10), its transition dipole, $H_{ki}^{(1)}$, and the mixing coefficients, $A_{ki}^{(\pm)}$. In the nonresonance region such as $h\omega=1.0$ eV, the polarizability decreases in the order of $K_2>Ag_2>MgO>Pd_2$. This order is the same as that of the transition dipole $H_{ki}^{(1)}$ for the main configuration, which is independent of the frequency. For Pd_2, the main configuration corresponds to the $d\rightarrow s$ excitation and the polarizability is the smallest in the nonresonance region, while for others, they are $s\rightarrow s$ or $s\rightarrow p$ type. Roughly speaking, since the transition from d to s orbitals is dipole-forbidden in the atomic case, the polarizabilities of the metals having the main configurations of $d\rightarrow s$ are smaller than that of $s\rightarrow p$. While the $s\rightarrow s$ transition in atoms is forbidden, the $s\sigma\rightarrow s\sigma^*$ transition in diatomics is dipole-allowed.

B. CO on Ag_2

Next, we investigate the polarizability and the SPD of the CO adsorbed on the Ag_2 cluster, in which the Ag–C distance is fixed at 2 Å. Figure 4 shows the five SPD curves of the Ag_2CO system calculated with the damping factors of 0, 0.01, 0.1, 0.3, and 1 eV, in comparing with that of the free CO molecule. The lifetimes of the excited state related to these damping factors are ∞, 6.6×10^{-14}, 6.6×10^{-15}, 2.2×10^{-15}, and 6.6×10^{-16} s, respectively. In Fig. 4, there is a peak at 1.63 eV for the SPD curve of $\Gamma=0$ eV, of which the tail to the lower and higher energy sides extends to 0.5 and 2.25 eV, respectively. The SPD value at the peak is about ten orders of magnitude larger than that of the free CO molecule. The enhancement decreases as the damping factor increases. Since the lifetime of the adsorbed molecule on the metal surface is reported to be of the order of 10^{-14}–10^{-13} s,[21] the corresponding Γ is around 0.01 eV. Thus, the maximum enhancement is estimated to be eight orders of magnitude larger than that of free CO even for this damping factor. However, the position of the peak does not agree with the experimental one at 2.25 eV (550 nm).[22] As shown later using the Ag_{10} cluster, this is mainly due to the use of the small metal cluster Ag_2.

We examine the dependence of the Raman intensity on the surface–adsorbate distance. Figure 5 shows the SPD curves of the Ag_2CO system calculated for the Ag–C distances of 2, 5, and 10 Å. The SPDs decrease drastically as the Ag–C distance increases, and no peaks are calculated for the SPD curves corresponding to the Ag–C distances of 5 and 10 Å. The SPD curve at 10 Å is very similar to that of the free CO molecule.

Table II shows both FDPs and SPDs of the Ag_2CO sys-

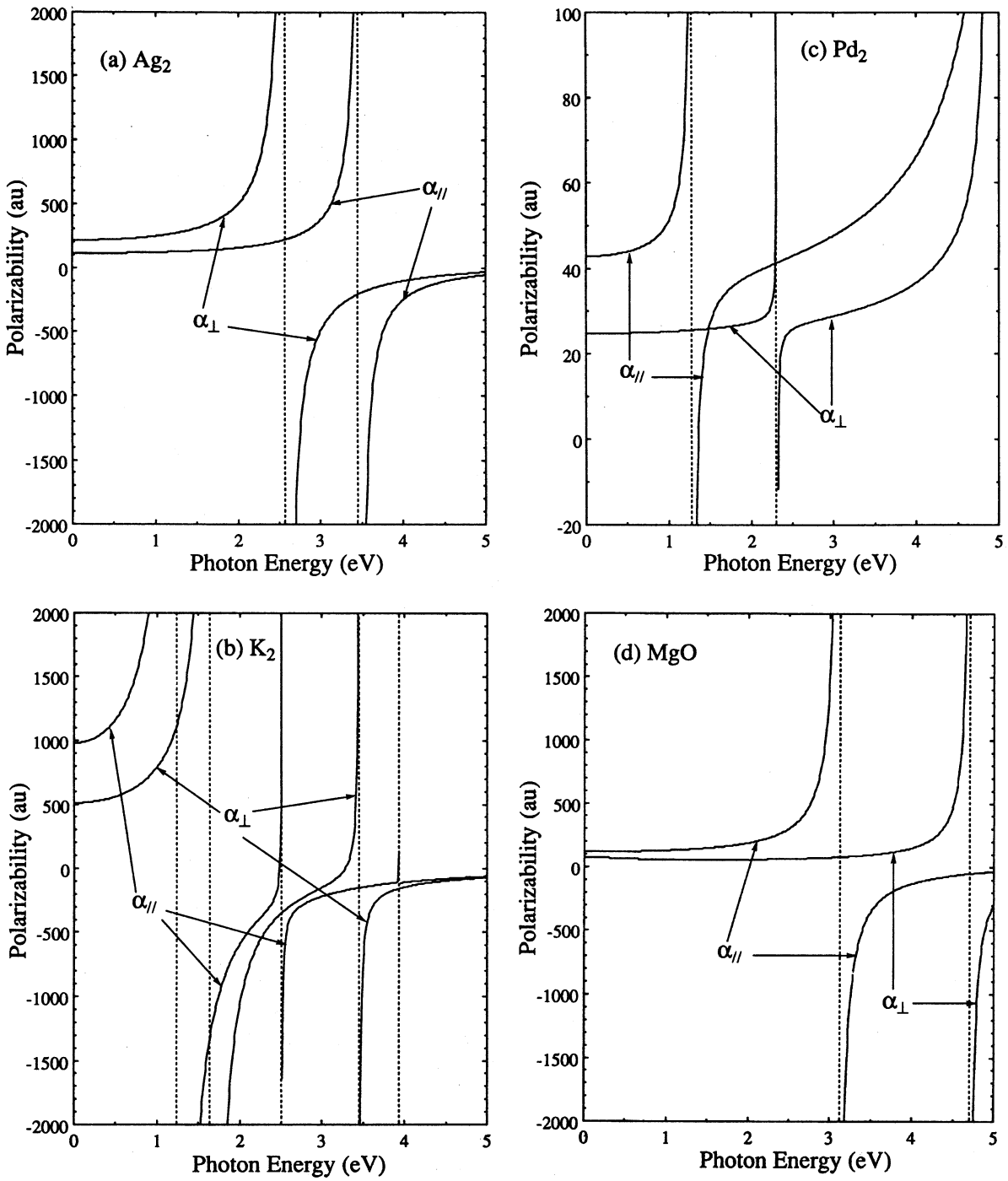

FIG. 3. Frequency dependence of the polarizabilities of the free (a) Ag_2, (b) K_2, (c) Pd_2, and (d) MgO calculated by the TDHF method.

tem for different Ag–C distances. Those of CO and Ag_2 are also shown in Table II, although the SPD with respect to the C–O distance is not defined or always zero in the Ag_2 molecule. While the FDP of the Ag_2CO system decreases as the Ag–C distance increases, the value approaches to that of Ag_2 plus CO rather than that of CO. On the other hand, the SPD becomes close to that of CO. These behaviors of the FDP and the SPD are quite natural and shows the reliability of the present method.

Figure 6 shows the SPD curve of the Ag_2CO with a different adsorbed geometry; that is, the oxygen atom of CO interacts with Ag_2 and the Ag–O distance is fixed to 2 Å. We call this geometry the O-on type and that in Figs. 4 and 5 C-on type. The SPD curves of the free CO and the C-on Ag_2CO are also shown in Fig. 6. The SPD of the O-on type is only one order of magnitude larger than that of CO in the nonresonance region, and the maximum value is four orders of magnitude smaller than that of the C-on type Ag_2CO. Furthermore, the resonance is seen in a smaller energy region, 2.1–2.4 eV, in comparison with the C-on Ag_2CO.

TABLE I. Polarizabilities of M_2 (M=Ag, K, Pd) and MgO at $h\omega=1.0$ eV.

Molecule	Direction	α	$i\rightarrow k$	$H_{ki}^{(1)}$	$A_{ki}^{(+)}$	$A_{ki}^{(-)}$	$\Delta E_{\text{SE-CI}}$
Ag_2	$\perp$	117.8	$5s\sigma\rightarrow 5p\pi$	1.98	−20.98	−29.34	$3.55(^1\Pi_u)$
	$\parallel$	243.7	$5s\sigma\rightarrow 5s\sigma^*$	2.58	−29.56	−50.20	$2.72(^1\Sigma_u^+)$
K_2	$\perp$	780.7	$4s\sigma\rightarrow 4p\pi$	3.13	−26.49	−216.40	$1.75(^1\Pi_u)$
	$\parallel$	2649.1	$4s\sigma\rightarrow 4s\sigma^*$	4.17	77.64	−709.81	$1.42(^1\Sigma_u^+)$
Pd_2	$\perp$	25.1	$4d\pi^*\rightarrow 5s\sigma^*$	0.30	−2.97	−3.96	$2.38(^1\Pi_u)$
	$\parallel$	50.6	$4d\sigma^*\rightarrow 5s\sigma$	0.36	−6.13	−15.25	$1.34(^1\Sigma_u^+)$
MgO	$\perp$	54.1	σ(O $2p$+Mg $3s$) $\rightarrow\pi^*$(Mg $3p$)	0.11	−25.88	−2.47	$4.93(^1\Pi)$
	$\parallel$	126.5	σ(O $2p$+Mg $3s$) $\rightarrow\sigma^*$(O $2p$+Mg $3s,3p$)	1.38	−9.77	−39.97	$3.73(^1\Sigma^+)$

These differences originate from the difference of the Ag_2–CO interactions.

The peak of the SPD curve is related to the lowest excited states of the Ag_2CO system, whose main configuration is the $5s\sigma$ to $5s\sigma^*(5p\sigma^*)$ excitation of Ag_2. The excitation energies of the C-on and O-on Ag_2CO are calculated to be 1.73 and 2.39 eV, respectively, by the SE-CI method. Since the corresponding excitation energy of the free Ag_2 molecule is 2.72 eV, the energy shift of the C-on molecule is larger than that of the O-on one. This difference shows a larger interaction between Ag_2 and CO in the C-on adsorption, which brings a larger enhancement of the Raman intensity.

Table III shows population analyses and net charges of the C-on and O-on Ag_2CO in the ground and the lowest excited states. Since the polarization d functions are used for C and O, the populations of the d orbitals are also shown in Table III. Q means the net charge and Δ means the difference between the values in the ground and excited states. Since the net charges on C and O do not change much by the lowest transitions in both cases, the resonance states do not correspond to the CT state between CO and Ag_2. The polarizations of Ag_2 in the ground state due to the CO adsorption are reduced by the excitations as seen in Table III; namely, from $Ag_a^{+0.139}$–$Ag_b^{-0.208}$ to $Ag_a^{-0.054}$–$Ag_b^{+0.053}$ in the C-on adsorption and from $Ag_a^{+0.155}$–$Ag_b^{-0.213}$ to $Ag_a^{-0.035}$–$Ag_b^{-0.028}$ in the O-on adsorption. This relaxation is mainly due to the changes of the Ag $5s$ and $5p_x$ populations, which are smaller in the C-on adsorption than those in the O-on one. On the other hand, the change in the $5p_z$ population of Ag_a, which is larger in the C-on adsorption than in the O-on one, is directly related to the SPD (zz) component parallel to the C–O axis. In fact, the transition

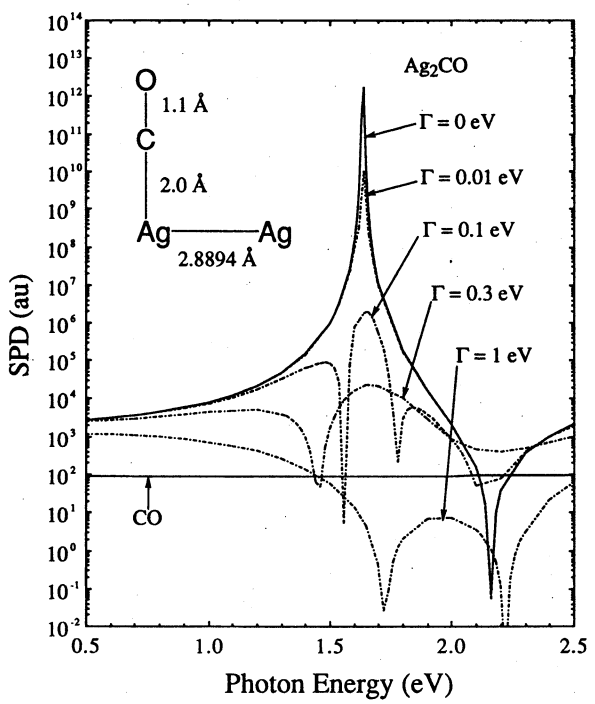

FIG. 4. Frequency dependence of the SPD for the C-on Ag_2CO system ($R=2$ Å) calculated with $\Gamma=0$, 0.01, 0.1, 0.3, and 1 eV.

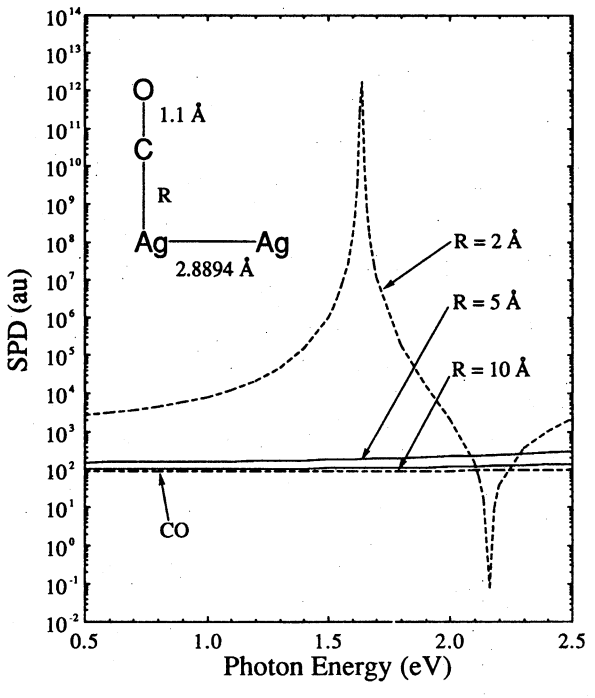

FIG. 5. Frequency dependence of the SPD in the C-on Ag_2CO system calculated with the Ag–C distances of 5 and 10 Å in comparison with $R=2$ Å.

TABLE II. Surface–adsorbate distance dependence of the FDP and the SPD in the Ag_2CO system.

		ω=1.0 eV		ω=1.5 eV		ω=2.0 eV		ω=2.5 eV	
System	R (Å)	FDP	SPD[a]	FDP	SPD[a]	FDP	SPD[a]	FDP	SPD[a]
Ag_2CO	2.0	228.6	6.52(+3)	442.7	5.85(+5)	819.4	2.81(+3)	147.2	1.84(+3)
	5.0	131.7	1.56(+2)	143.9	1.75(+2)	166.7	2.17(+2)	214.4	3.10(+2)
	10.0	125.2	9.90(+1)	137.8	1.04(+2)	161.8	1.13(+2)	213.5	1.36(+2)
CO		12.3	8.58(+1)	12.4	8.73(+1)	12.5	8.94(+1)	12.5	9.21(+1)
Ag_2		117.8		130.6		155.1		208.2	

[a]Powers of ten are shown in parentheses.

dipole moment $H_{ki}^{(1)}$ of the main $5s\sigma \rightarrow 5s\sigma^*$ configuration is 1.02 a.u. in the C-on system and 0.60 a.u. in the O-on system, though that in the free Ag_2 molecule is zero. Therefore, the mixing of the $5p_z$ AO to the $5s\sigma$ MO, which is induced by the CO adsorption, is important for the SERS. It is also noted that the changes in the $4d$ populations of Ag_a and Ag_b are much smaller than those in $5s$ and $5p$ populations.

C. CO on Ag_{10}

We next examine CO molecule adsorbed on a larger cluster, Ag_{10} as a model of the Ag(100) surface as illustrated in Fig. 7. The numbers of the Ag atoms in the first, second, and third layers are 5, 4, and 1, respectively. CO interacts directly with the central Ag atom in an end-on form with the distance of 2 Å. Since the d orbitals are found to be inactive for the SERS effect in the previous section, we use the one-electron ECP and $[3s2p]$ set[23] for the silver atoms except for the central Ag atom, for which the 11-electron ECP and $[3s2p2d]$ set[17] are used. This $Ag_{10}CO$ system should be more realistic than the Ag_2CO system for the present purpose.

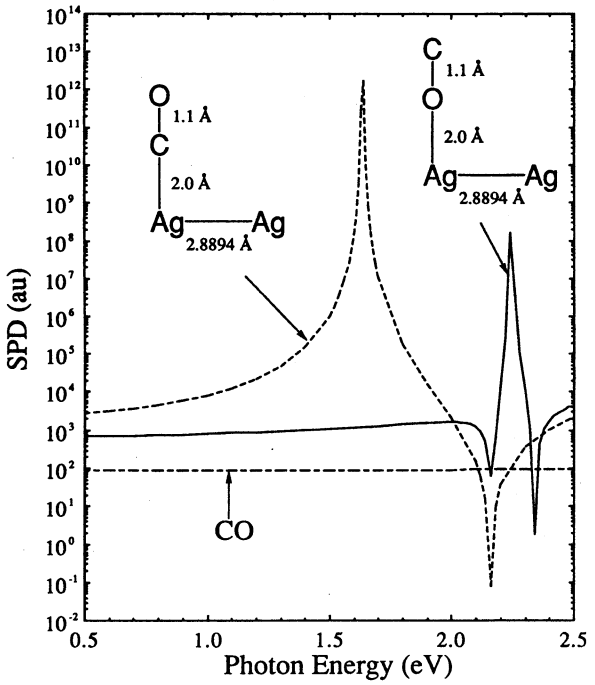

FIG. 6. Frequency dependence of the SPD in the O-on Ag_2CO system in comparison with the C-on one.

The SPD curves with Γ=0 and 0.01 eV are shown in Fig. 7 by the solid and dotted-broken lines, respectively. For comparison, we show the SPD curves of the free CO molecule by the broken lines. In Fig. 7, there is a peak at 2.23 eV for the SPD curve of Γ=0 eV. This peak is broad and the intensity is still very large even when Γ=0.01 eV. The SPD value at the peak is about seven orders of magnitude larger than that of the free CO molecule.

This peak of the SPD curve is related to the 2 $^1A_1$ excited states of the $Ag_{10}CO$ system, whose main configuration is the inner excitation of the Ag_{10} cluster. Table IV shows the population analysis and the net charge of the C and O atoms of $Ag_{10}CO$ in the 1 $^1A_1$ ground and the 2 $^1A_1$ excited states. Since the net charges on C and O do not change much by the 1 $^1A_1 \rightarrow 2\ ^1A_1$ transition, the resonance states do not correspond to the CT state between CO and Ag_{10}. It shows that the SERS is mainly due to the polarization of the metal cluster and not due to the CT effect between the cluster and the admolecule. In this point, which is the most important result of this study, the previous result with the Ag_2CO system is valid.

The experimental spectrum showing the wavelength dependence of the Raman intensity observed by Moskovits *et al.*[22] is inserted into Fig. 7. The experimental spectrum has a peak near 550 nm, namely 2.35 eV. The present theoretical spectrum with the $Ag_{10}CO$ system has a peak at 2.23 eV, so that it reproduces well both of the intensity and the peak position of the experimental spectrum. As already shown, the peak position calculated with the Ag_2CO system does not agree with the experiment. We therefore conclude that the metal dimers are sufficient to represent the SERS effect of a solid surface, though it does not well reproduce the peak position of the SERS.

D. CO on K_2, Pd_2, MgO, Ar

Finally, we examine CO molecule adsorbed on different solid clusters, namely, K_2, Pd_2, MgO, and Ar, for which the M–C distances used in the calculations are 3, 2, 2, and 2.4 Å, respectively. Since both C-on and O-on adsorptions of CO are observed on the MgO surface, we calculate the SPDs of both geometries. The SPD curves with Γ=0 and 0.01 eV are shown in Fig. 8 by the solid and the dotted-broken lines,

TABLE III. AO population analysis and the net charge Q for the ground and the lowest excited states of the C-on and O-on Ag_2CO systems.

State	C				O				Ag_a					Ag_b				
	s	p	d	Q	s	p	d	Q	s	p_x	p_y	p_z	d	Q	s	p_x	p_y	p_z	d	Q
C-on adsorption																				
Ground	3.568	2.148	0.186	+0.098	3.717	4.281	0.031	−0.029	0.663	0.190	0.006	0.175	9.818	+0.139	1.235	0.047	0.002	0.002	9.923	−0.208
Excited	3.543	2.229	0.183	+0.045	3.714	4.300	0.031	−0.044	0.463	0.661	0.003	0.133	9.794	−0.054	0.926	0.070	0.003	0.025	9.923	+0.053
Δ	−0.025	+0.081	−0.003	−0.053	−0.003	+0.019	0.000	−0.015	−0.200	+0.462	−0.003	−0.042	−0.024	−0.193	−0.309	+0.023	+0.001	+0.023	0.000	+0.261
O-on adsorption																				
Ground	3.722	1.971	0.146	+0.161	3.677	4.388	0.037	−0.102	0.748	0.089	0.006	0.070	9.933	+0.155	1.221	0.048	0.002	0.001	9.941	−0.213
Excited	3.724	1.950	0.146	+0.179	3.672	4.407	0.037	−0.116	0.344	0.722	0.007	0.057	9.906	−0.035	0.819	0.266	0.003	0.016	9.923	−0.028
Δ[a]	+0.002	−0.021	0.000	+0.018	−0.005	+0.019	0.000	−0.014	−0.404	+0.633	+0.001	−0.013	−0.027	−0.190	−0.402	+0.218	+0.001	+0.015	−0.018	+0.185

[a]The difference between the ground- and excited-state values.

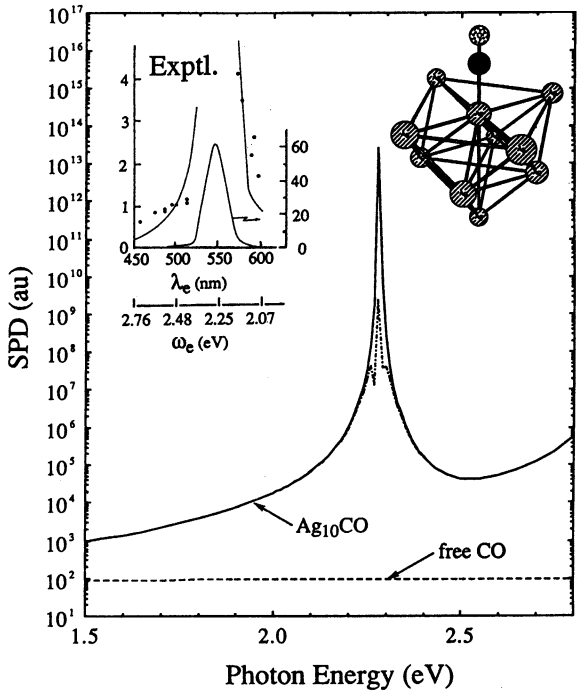

FIG. 7. Frequency dependence of the SPDs in the $Ag_{10}CO$ system. The solid and dotted-broken lines are the results for $\Gamma=0$ and 0.01 eV, respectively. The broken line shows the SPD for free CO. The inserted figures are the illustrated geometry of the $Ag_{10}CO$ system and the experimental spectrum for the wavelength dependence of the Raman intensity observed by Moskovits *et al.* (Ref. 22).

respectively. For comparison, we also show the SPD curves of CO adsorbed on Ag_2 with $\Gamma=0$ eV and of the free CO by the broken lines.

The SPD curves of the K_2CO system have four peaks in the energy region from 0.5 to 2.5 eV. Among them, the three peaks at 1.09, 2.01, and 2.44 eV are sharp but reduced much when Γ is modified from 0 to 0.01 eV. On the other hand, the peak at 1.66 eV is broad and the intensity is still very large even when $\Gamma=0.01$ eV. The SPDs of the Pd_2CO system are smaller than those of the Ag_2CO and K_2CO systems. Three peaks at 1.89, 2.04, and 2.15 eV are sharp and the reduction at $\Gamma=0.01$ eV is large. For the two MgO(CO) systems, the C-on adsorption shows a larger enhancement than the O-on one, as observed for the Ag_2CO system. The two SPD curves for $\Gamma=0$ and 0.01 eV overlap in the O-on MgO(CO) system. The maximum enhancement factors of the Raman intensities of the CO on K_2, Ag_2, MgO, and Pd_2 are nine, eight, five, and one, respectively. This order is the same as that of the polarizabilities of the free clusters. Argon matrix is sometimes used to observe the Raman scattering of the adsorbed molecule. Actually, the calculated SPD curve of the ArCO system is very similar to that of the free CO molecule, as shown in Fig. 8(d), which supports that the effect of the matrix is very small and negligible for the SERS.

The present results show that the SERS originates from the surface polarization and the interaction between the adsorbate and the surface plays a key role for coupling the surface polarization and the adsorbate vibrations. The en-

TABLE IV. AO population analysis and the net charge Q of C and O for the $1\ ^1A_1$ ground and the $2\ ^1A_1$ excited states of the $Ag_{10}CO$ system.

	C				O			
State	s	p	d	Q	s	p	d	Q
$1\ ^1A_1$ (Ground)	3.578	2.104	0.178	+0.140	3.727	4.289	0.030	−0.046
$2\ ^1A_1$ (Excited)	3.555	2.121	0.179	+0.145	3.729	4.273	0.030	−0.032
Δ[a]	−0.023	+0.018	+0.001	+0.005	+0.002	−0.016	0.000	+0.014

[a]The difference between the ground- and excited-state values.

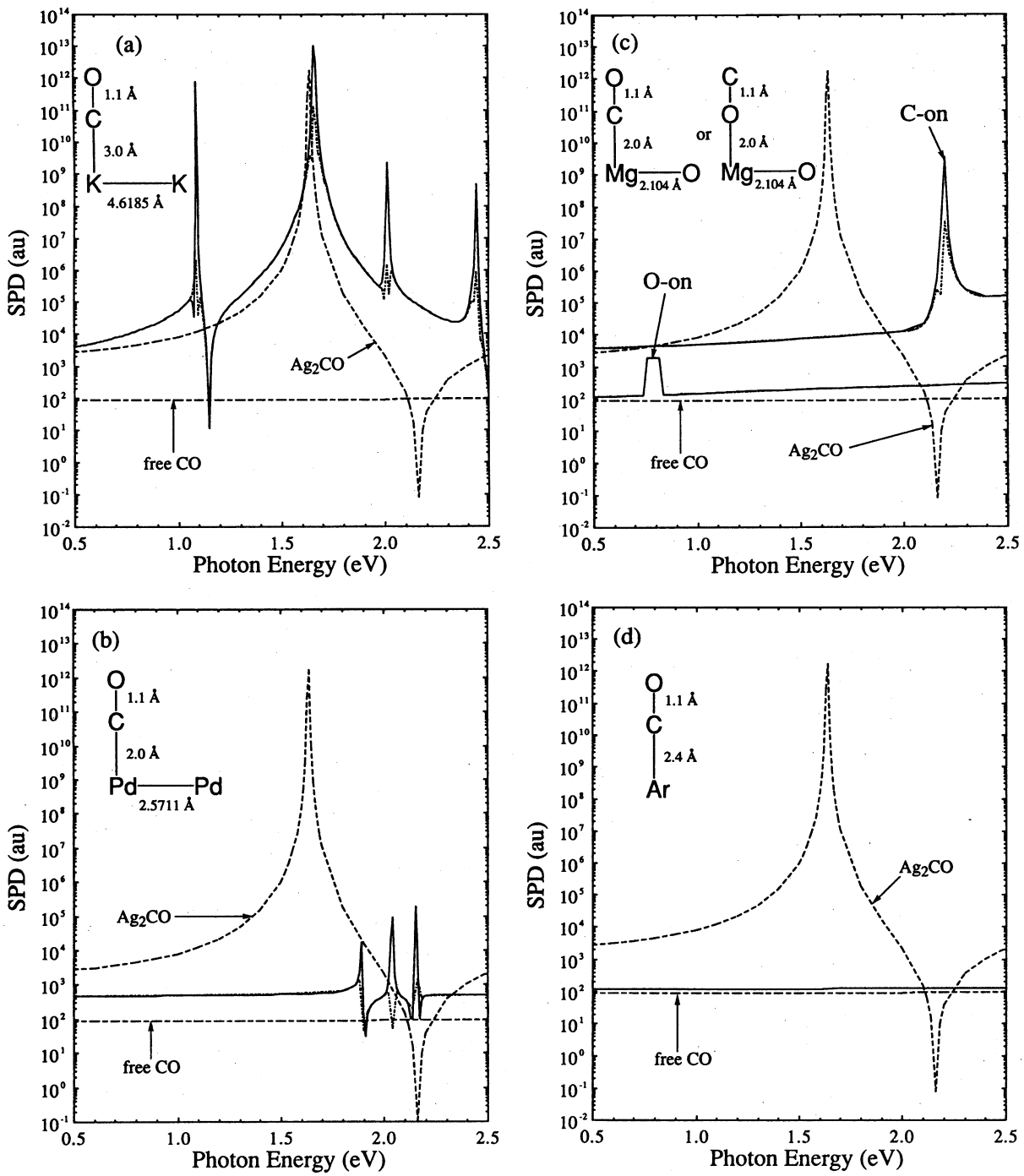

FIG. 8. Frequency dependence of the SPDs in (a) K_2CO; (b) Pd_2CO; (c) MgO(CO); and (d) ArCO systems. The solid and dotted-broken lines are the results for $\Gamma=0$ and 0.01 eV, respectively. Two broken lines show the SPDs for free CO and for the C-on Ag_2CO system.

hancement is related to the polarizability of the free solid cluster, which are also related with the conductivity or the dielectric constant of the solid surface. Furthermore, the enhancement depends on the distance and the orientation of the surface–adsorbate system.

IV. CONCLUDING REMARKS

In this study, we have tried to clarify the electronic mechanism of the SERS by *ab initio* MO theory. We investigate the Raman intensities of CO adsorbed on solid clusters such as Ag_2, Ag_{10}, K_2, Pd_2, and MgO, which represent the surface effect. The TDHF method has been applied to the calculations of the polarizability and the finite difference approximation has been used for calculating the derivative of the polarizability with respect to the vibrational coordinate.

The maximum intensity of CO on the Ag_2 cluster is calculated to be ten orders of magnitude larger than that of the free CO molecule. The enhanced intensity decreases with the increase of the damping constant which is inversely proportional to the lifetime of the excited state. With the damping constant of 0.01 eV, which corresponds to the lifetime of the excited state of the molecule adsorbed on a metal surface, the calculated enhancement factor is still eight in comparison with the experimental ones of four to eight. The wavelength dependence of the Raman intensity calculated with the $Ag_{10}CO$ system agrees well with the experimental spectrum in both intensity and peak position, but that with the smaller Ag_2CO system does not reproduce the peak position.

The present study shows that the resonance transition due to the surface polarization is essential for a large enhancement of the Raman intensity of the adsorbed molecule. Therefore, the enhancement is related to the polarizability of the free solid cluster, which corresponds to the conductivity or the dielectric constant of the solid surface. The resonance state does not have the charge-transfer nature between the surface and the molecule. However, the surface–molecule interaction is also important for SERS, and therefore the enhancement is greatly dependent on the orientation of the molecule and on the distance from the surface.

ACKNOWLEDGMENTS

Part of this study has been supported by the Grant-in-Aid for Scientific Research from the Japanese Ministry of Education, Science, and Culture.

[1] M. Fleischmann, P. J. Hendra, and A. J. McQuillian, Chem. Phys. Lett. **26**, 163 (1974).
[2] R. K. Change and T. E. Furtak, *Surface Enhanced Raman Scattering* (Plenum, New York, 1982).
[3] R. L. Birke and J. R. Lombardi, *Advances in Laser Spectroscopy*, edited by B. Garetz and J. R. Lombardi (Heyden, Philadelphia, 1982), Vol. 1, p. 143.
[4] T. E. Furtak, *Advances in Laser Spectroscopy*, edited by B. Garetz and J. R. Lombardi (Heyden, Chichester, 1984), Vol. 2, p. 175.
[5] R. K. Change and B. L. Laube, *CRC Critical Reviews in Solid State and Materials Science* (Chemical Rubber, Boca Raton, Florida, 1984), Vol. 12, p. 1.
[6] A. Otto, *Light Scattering in Solids*, edited by M. Cardona and G. Guntherodt (Springer, Berlin, 1984), Vol. IV.
[7] For example, H. Nakatsuji and H. Nakai, Chem. Phys. Lett. **174**, 283 (1990); J. Chem. Phys. **98**, 2423 (1993).
[8] A. Dalgarno and G. A. Victor, Proc. R. Soc. A **291**, 291 (1966).
[9] P. W. Langhoff, S. T. Epstein, and M. Karplus, Rev. Mod. Phys. **44**, 602 (1972).
[10] D. P. Santry and T. E. Raidy, Chem. Phys. Lett. **61**, 413 (1979).
[11] P. K. K. Pandey and G. C. Schatz, Chem. Phys. Lett. **88**, 193 (1982); **91**, 286 (1982).
[12] H. A. Kramers and W. Heisenberg, Z. Phys. **31**, 681 (1925).
[13] P. A. M. Dirac, Proc. R. Soc. London, Ser. A **114**, 710 (1927).
[14] G. Placzek, *Handbuch der Radiologie* (Akademische, Leipzig, 1934), Vol. VI.
[15] L. E. Sutton, *Tables of Interatomic Distances and Configuration in Molecules and Ions* (Royal Society of Chemistry, London, 1965).
[16] M. Dupuis, J. D. Watts, H. O. Viller, and G. J. B. Hurst, Program Library HONDO7 (No. 1501), Computer Center of the Institute for Molecular Science, 1989.
[17] P. J. Hay and W. R. Wadt, J. Chem. Phys. **82**, 271 (1985).
[18] W. R. Wadt and P. J. Hay, J. Chem. Phys. **82**, 284 (1985).
[19] S. Huzinaga, J. Andzelm, M. Klobukowski, E. Radzio-Andzelm, Y. Sakai, and H. Tatewaki, *Gaussian Basis Sets for Molecular Calculations* (Elsevier, New York, 1984).
[20] S. Huzinaga, J. Chem. Phys. **42**, 1293 (1965); T. H. Dunning, Jr., *ibid.* **53**, 2823 (1970).
[21] J. W. Gadzuk, Surf. Sci. **184**, 483 (1987).
[22] D. P. DiLella, A. Gohin, R. H. Lipson, P. McBreen, and M. Moskovits, J. Chem. Phys. **73**, 4282 (1980).
[23] P. J. Hay and R. L. Martin, J. Chem. Phys. **83**, 5174 (1985).